Available online at www.sciencedirect.com
SCIENCE DIRECT®

Applied Radiation and Isotopes 62 (2005) 457–460

Applied Radiation and Isotopes

www.elsevier.com/locate/apradiso

Neutron-induced electron radiography using an imaging plate

R. Pugliesi[a,*], E. Lehmann[b]

[a]Instituto de Pesquisas Energeticas e Nucleares (IPEN-CNEN/SP), Cidade Universitária, Av. Prof. Lineu Prestes 2242, Butantã, CEP 05508-000 São Paulo SP, Brazil
[b]Paul Scherrer Institut, CH-5232 Villigen PSI, Switzerland

Received 9 April 2004; received in revised form 17 June 2004; accepted 30 June 2004

Abstract

Neutron-induced electron radiography is a technique suitable for inspection of thin samples. The first tests were performed with conventional X-ray films, which made it possible to distinguish between thicknesses of materials of the order of 1 μm. The objective of this work was to investigate the performance of the technique when an imaging plate is used instead of an X-ray film to register the image. Due to their wide dynamic range and much higher sensitivity, imaging plates offer significant advantages over the conventional X-ray films.

Keywords: Electron radiography; Neutron induced; Neutron converter; Imaging plate; Attenuation coefficient; Thin layers; Detection limit

1. Introduction

Neutron-induced electron radiography (NIER) is a new non-destructive testing technique (Pugliesi, 2001). It inspects the internal structure of thin sample layers (of the order of a few micrometers) using a low-energy electron field as penetrating radiation. This technique turns out to be very useful in inspecting, for example, documents and thin biological samples. The radiation source of the electronic field is a gadolinium metal foil, which provides low-energy 70 keV conversion electrons under irradiation with thermal neutrons (Hawkesworth and Walker, 1969). Radiographs are obtained with an aluminum cassette containing a conventional X-ray film, a sample to be inspected, and the gadolinium metal foil (in this order in the direction of the neutron beam); these constituents are kept in a tight contact during neutron irradiation. The neutron beam passes through the film, then through the sample, and, finally, induces (n,γ) reactions in the gadolinium foil. The generated electron beam goes back through the sample and selectively sensitizes the film, which can then be developed using standard procedures to produce an image. The film image is evaluated on a negatoscope, where the levels of sensitization are measured with an optical densitometer. The levels vary from 0 (direct beam light) to about 4 (dark image).

The objective of this work was to investigate the sensitivity of the NIER technique when an imaging plate (IP) sensitive to ionizing radiation (Kobayashi, 1998) is used instead of the conventional X-ray film and to compare the results with those obtained in our previous work (Pugliesi, 2001). The main reasons to employ an IP were its wide dynamic range, high sensitivity, and the ability to directly provide radiographic images in a digital form.

2. Experimental

The irradiations were performed at the neutron radiography facility NEUTRA installed at the Spalla-

*Corresponding author. Tel.: +55-11-3816-9178; fax: 55-11-3816-9188.
E-mail address: pugliesi@curiango.ipen.br (R. Pugliesi).

0969-8043/$ - see front matter
doi:10.1016/j.apradiso.2004.06.011

tion Neutron Source SINQ of the Paul Scherrer Institute (Lehmann et al., 2000). This neutron beam has a negligible gamma radiation component, and its main characteristics at the gadolinium foil position are shown in Table 1.

As proposed in the previous paper (Pugliesi, 2001), the irradiations were performed in a cassette containing the IP, the sample, and the gadolinium metal foil (in this order in the direction of the neutron beam) kept in a tight contact. The experimental setup is schematically shown in Fig. 1. The IP BAS-MP was manufactured by Fuji; the gadolinium foil was 25 μm thick. After the neutron beam application and the exposure of the IP to induced electrons, the plate was de-excited by a scanning laser, and the emitted light formed a 16-bit digital image with 50 μm pixels. The quantification in a gray-level (GL) scale was performed in such a way that the darkest pixel corresponded to the level zero, while the lightest was represented by level 65536. In these studies, the irradiation time was 5 min under the conditions listed in Table 1.

The sensitivity of the technique to thickness was investigated for four different materials. The samples were step wedges with thicknesses varying in the following ranges:

- aluminum foil—from 10 to 100 μm;
- polymer "Makrofol KG"—from 10 to 100 μm;
- adhesive tape—from 50 to 250 μm;
- ordinary white paper—from 100 to 400 μm.

Table 1
Characteristics of the NEUTRA facility neutron beam at the gadolinium foil

Thermal flux intensity ($ns^{-1} cm^{-2}$)	3×10^6
Beam diameter (cm)	40
Mean energy (meV)	25

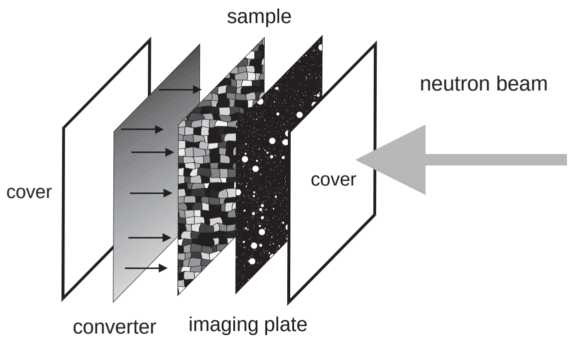

Fig. 1. Setup of the NIER experiment, where the neutron beam is converted into the electron radiation detected by an imaging plate.

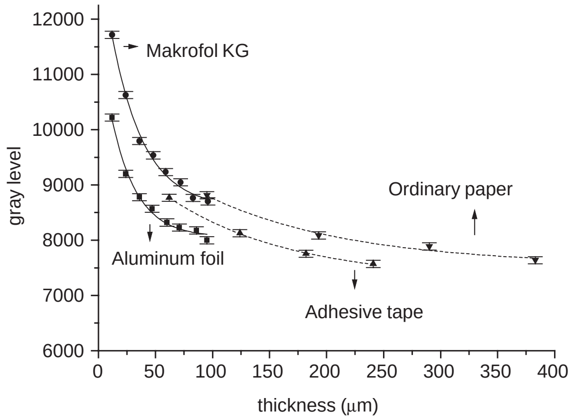

Fig. 2. Gray-level intensity as a function of the sample thickness for aluminum foil, Makrofol KG, adhesive tape, and ordinary paper.

The radiographic images were scanned, and the obtained gray-level intensities as functions of the sample thicknesses are shown in Fig. 2. These experimental data are best fitted with an exponential function

$$GL(x)A + B\,e^{-C\cdot x}, \tag{1}$$

where A, B, and C are variable parameters of the fit, and x is the sample thickness. The thickness sensitivity, or the minimal detectable thickness change was calculated for various thicknesses using the derivative of Eq. (1) according to Hardt and Rotteger (1981):

$$\Delta x = -\frac{\Delta \min(\mathrm{GL})}{BC\,e^{-C\cdot x}}, \tag{2}$$

where Δmin(GL) is the minimal detectable gray-level intensity in the image.

The plots of the sensitivity values as functions of the sample thickness are shown in Fig. 3.

3. Analysis

In the present work, the "neutron → IP → sample → Gd foil" irradiation geometry was the same as in the previous work described by Pugliesi (2001), which ensured that most of the generated electrons reach the sample.

The exponential fit to the gray-level intensity as a function of the sample thickness is just empirical, because, for these conditions, neither the electron spectra generated by the gadolinium foil, nor the law controlling the electron transmission by these materials were determined.

As evaluated from Eq. (2), the method was able to detect a thickness difference of ~0.7 μm in 10 μm

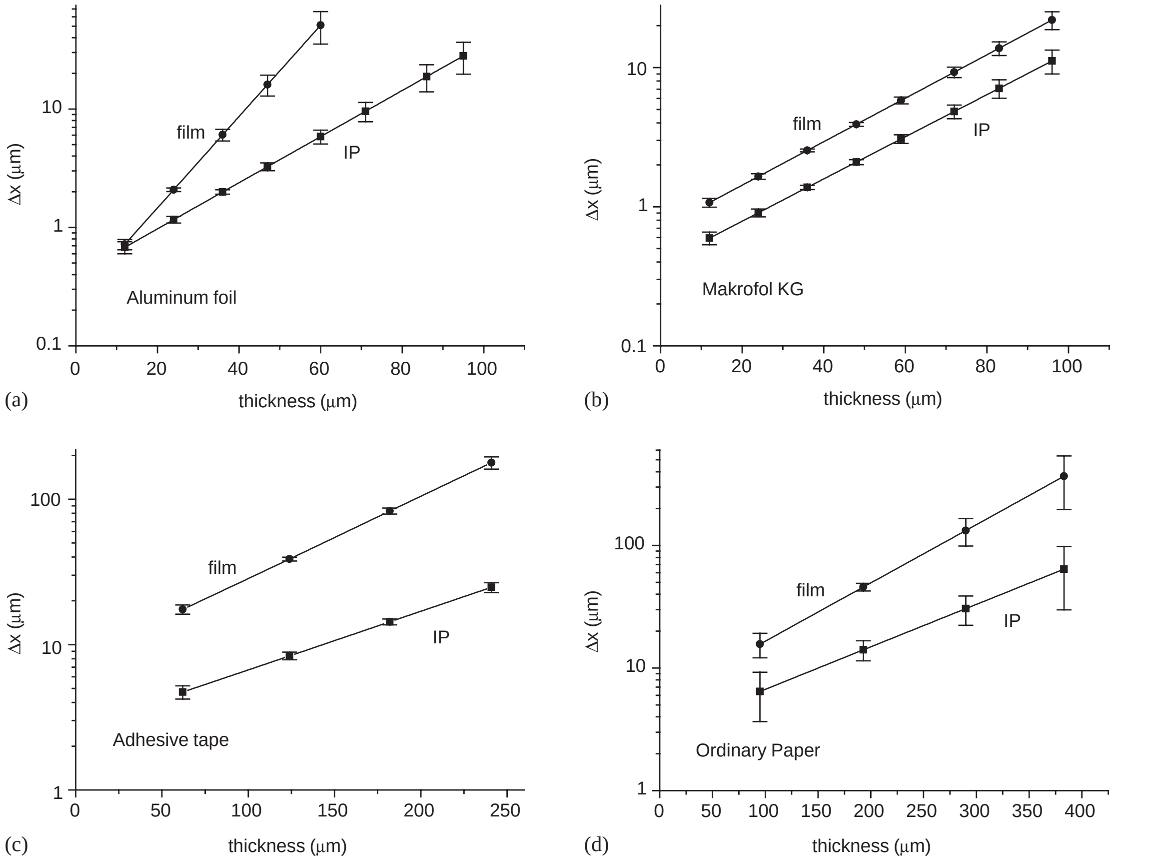

Fig. 3. NIER sensitivity as a function of the sample thickness for: aluminum foil (a), Makrofol KG (b), adhesive tape (c), and ordinary paper (d).

aluminum foil, of ~0.6 μm in 10 μm film of polymer Makrofol-KG, of ~4 μm in 50 μm adhesive tape, and of ~6 μm in 100 μm ordinary paper.

Fig. 3 shows relative sensitivities of the NIER technique with IP and the conventional X-ray film. Clearly, due to its wider dynamic range, IP has improved the sensitivity to thickness differences.

We have also evaluated the minimal detectable thickness (which represents the minimal amount of material that can be detected) and the effective attenuation coefficients for the studied materials; Table 2 shows the results. The former was calculated by extrapolating the function (2) to $x = 0$, and the latter is the value of the constant C in Eq. (1).

For comparison, Table 2 also provides the minimal detectable thickness for the standard thermal neutron radiography (NR) technique with a film/Gd set and effective macroscopic cross sections (Σ) for some highly thermal-neutron absorbing materials, such as gadolinium, cadmium, and gold (Berger, 1998).

It is important to note that, after the maximal range of the 70 keV electrons is reached in a sample, the capability of the method to detect thickness changes will get worse, because the image will be formed by the less intense 150 keV conversion electrons and the 70 keV gamma-rays emitted by gadolinium nuclei. This can be seen in the case of aluminum foil (Fig. 2), for which the

Table 2
Comparison of the performance characteristics of NIER and the standard NR technique

	Material	Minimal thickness (μm)	C (cm^{-1})
NIER			
	Aluminum foil	0.39 ± 0.07	450 ± 49
	Makrofol-KG	0.39 ± 0.06	351 ± 35
	Adhesive	2.7 ± 0.4	94 ± 9
	Paper	3 ± 2	79 ± 32
NR			Σ (cm^{-1})
	Gadolinium	0.2	1354
	Cadmium	2	136
	Gold	63	4.65

The right column contains parameters C in Eq. (1) for the materials under investigation and the effective macroscopic cross-sections Σ for some typical strong thermal neutron absorbers.

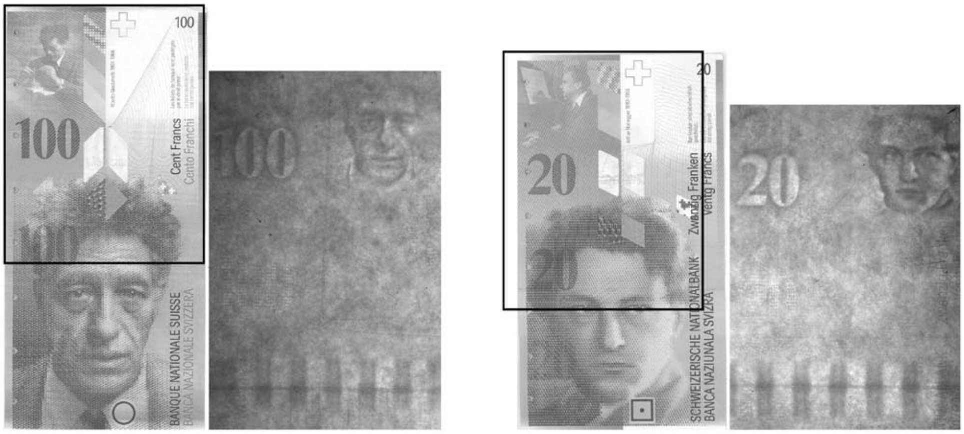

(a) (b)

Fig. 4. Neutron-induced electron radiographs of Swiss currency: a 100 CHF bill (a); a 20 CHF bill (b). The NIER images (right) correspond to the areas marked on the bill photographs (left). The NIER images exhibit mainly the water proofs and other density fluctuations of the paper.

range of the 70 keV electrons is about 40 μm. The intensity decreases not as rapidly for the thicknesses greater than 40 μm.

4. Conclusions

The NIER is a very promising technique for inspecting internal structures of thin samples with thickness in the μm range.

The effective attenuation coefficients for the studied materials obtained with the NIER method are of the same order of magnitude as the effective macroscopic cross-sections for some of the strongest thermal neutron absorbers in conventional NR. Hence, the capability of the former technique to distinguish between similar thicknesses is as high as of the latter.

If a standard neutron radiography facility is available, the cost of using the NIER method is very low, because most of the existing infrastructure, such as the neutron beam, shielding, converter screens, and cassettes, can be used.

Either with imaging plates or with conventional X-ray films, the technique is able to detect small thickness changes. However, because of the wider dynamic range, the capabilities of the former are stronger (Fig. 3).

In order to demonstrate some possible applications of this methodology, we inspected some regular Swiss bills with NIER, and the results are shown in Fig. 4. The image visualization was enhanced by means of the standard digital image processing procedures. It was easy to observe some of the impressed security marks; nothing would be visible with the conventional neutron radiography.

References

Berger, H., 1998. Neutron radiography—a state of art report. NTIAC–SR–98–. NASA (Center for Aerospace Information).

Hardt, P., Von, Der., Roettger, H., 1981. Neutron Radiography Handbook: Nuclear Science and Technology, D. Reidl, Dordrecht.

Hawkesworth, M.R., Walker, J., 1969. Radiography with neutrons. Rev. J. Mater. Sci. 4, 817–835.

Kobayashi, H., 1998. Basic performance of a neutron sensitive photostimulated luminescence device for neutron radiography. In: Proceedings of the Third International Topical Meeting on Neutron Radiography, Lucerne, Switzerland.

Lehmann, E., Vontobel, P., Wiezel, L., 2000. Properties of the radiography facility NEUTRA at SINQ and its use as European reference facility. Nondestr. Test. Eval. 16, 191–202.

Pugliesi, R., 2001. Progress of neutron radiography at the IEA-R1 nuclear research reactor (Last 15 Years). Meeting of the Advisory Group for Development and Application of Neutron Radiography. International Atomic Energy Agency (IAEA), Vienna.